INT. J. NUM. HEAT FLUID FLOW, VOL. 2, 469–476 (1992)

THREE-DIMENSIONAL SIMULATION OF THE HEAT TRANSFER AND TEMPERATURE DISTRIBUTION IN A LIQUID GAS TANK

J. A. VISSER and H. ROLFES

Department of Mechanical Engineering, University of Pretoria, Pretoria, 0002, South Africa

ABSTRACT

By modelling the unsteady heat transfer in liquid gas tanks, the temperature distribution in the tank as well as the heat flux reaching the liquid gas can be predicted. Knowledge of the temperature distribution and heat flux can be used to predict evaporation losses from the tank. By minimizing the evaporation losses, the thermal design of a gas tank can be optimized. This paper presents a finite difference simulation of the unsteady three-dimensional heat transfer in gas tanks and an optimized configuration. The numerical procedure accounts for radiation from the sun as well as radiative and convective heat transfer with the environment. A non-uniform grid is used because the tank consists of several different materials of varying dimensions and properties. Geometrical effects such as variations in the thickness of the insulation material and the diameter and height of the tanks are also studied in an attempt to optimize the design configuration.

KEY WORDS Liquid gas tanks Thermal optimization Finite difference simulation

NOMENCLATURE

A	surface area for heat transfer (m^2)
a	coefficient in discretized equation (W/K)
b	source term in the discretization equation (W)
C	specific heat capacity of the material (J/kgK)
C_c	empirical constant
d	tank diameter (m)
G	solar radiation intensity (W/m^2)
Gr_f	Grashof number for natural convection
h	convection heat transfer coefficient (W/m^2K)
h_r	radiation heat transfer coefficient (W/m^2K)
k	thermal conductivity value of the surrounding air (W/mK)
k_{int}	interface thermal conductivity (W/mK)
k_1, k_2	thermal conductivities of materials (W/mK)
m	empirical constant
Nu_f	Nusselt number evaluated at fluid temperature
Pr_f	Prandtl number evaluated at fluid temperature
Q	total heat flux (W)
r, ϕ, z	space co-ordinates in cylindrical system (m)

0961–5539/92/050469–08$2.00

Received August 1991
Revised April 1992

T	temperature (K)
ε	emissivity
ρ	material density (kg/m^3)
τ	time (sec)

Subscripts

np	general neighbouring grid point
p	central grid point under consideration
s	evaluated at the surface
t	current configuration
∞	evaluated at environmental conditions

INTRODUCTION

Several gases such as nitrogen, oxygen and argon are frequently used for different industrial applications. Owing to the large quantities of gas required, the gas is liquefied to reduce the volume needed for storage. As a liquid, the temperature of the gas is much lower than the ambient temperature. Heat is therefore constantly transferred to the liquid gas which causes evaporation losses from the storage tanks. The present competitive market is forcing distributors of liquid gases to minimize evaporation losses in order to reduce the consumer price. This can be achieved by optimizing the thermal design of the storage tanks.

The thermal optimization of a liquid gas tank includes several important aspects of which the most important is the reduction of the heat flux to the liquid gas. The designer must further ensure that no ice will accumulate on the outer surface of the tank during cold winter nights. The temperature on the inside of the concrete slab must also be high enough to prevent embrittling of the concrete. To achieve these goals, complete information of the temperature distribution through the tank and the resultant heat transfer is required. The unsteady three-dimensional heat transfer problem cannot be solved analytically, resulting in the development of a numerical model.

A literature survey did not reveal any publications on the numerical prediction of heat flux to, or temperature distributions in liquid gas tanks. Several similar unsteady problems had, however, been solved in the past, using numerical simulations. A number of papers present one-dimensional and two-dimensional models[1–3] for predicting unsteady heat transfer and temperature distributions. Fu *et al.*[4] presented a three-dimensional model with which the time-varying temperature distribution in composite material bridges can be predicted. Van der Walt *et al.*[5] used a similar numerical technique to predict the temperature distribution in steel bars during reheating. The model is limited to a homogeneous material and a fixed grid and could therefore not be used to model a gas tank consisting of several different materials. Visser[6] developed a two-dimensional model for predicting temperature distribution in bodies consisting of different materials and using a variable grid. This model formed the basis for the development of the present numerical model.

This paper outlines a numerical method for predicting the three-dimensional unsteady heat transfer and the resultant temperature distribution and heat flux in liquid gas tanks.

CONFIGURATION OF A GAS TANK

A schematic representation of the construction of a liquid gas tank is shown in *Figure 1*. The tank is constructed on a reinforced concrete base about one metre above ground level. Several layers of foam glass are built on top of this concrete slab to support the liquid gas tank. Possessing good insulation characteristics, the foam glass also serves to insulate the inner tank from the environment. A stainless steel tank, in which the liquid is stored, is positioned on top of the

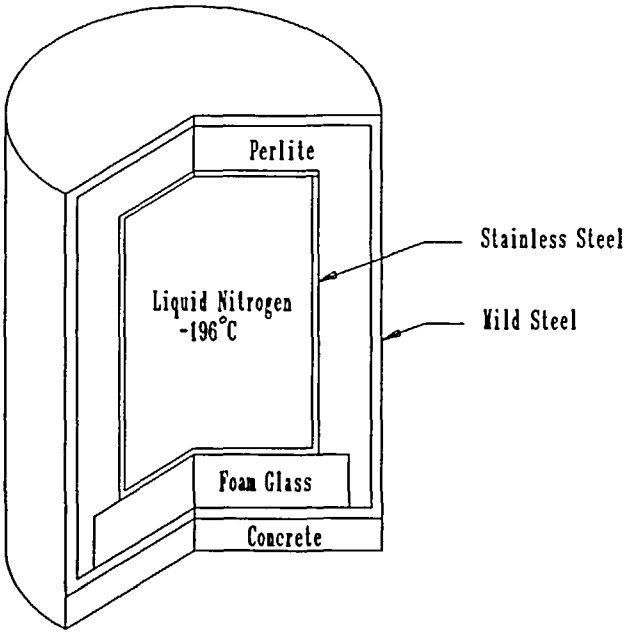

Figure 1 Schematic representation of a liquid gas tank

foam glass. A thick layer of Perlite insulates the inner tank along the top and sides. The entire construction is enclosed in a steel drum. The dimensions of such a drum are typically 16 m in diameter and 20 m high.

OUTLINE OF THE MODELLING PROCEDURE

Generation of the grid

The size of the grid representing a specific tank depends mainly upon the construction, composition and dimensions of the gas tank. Grid sizes were varied for the different materials in the tank to ensure adequate grid cells in each of the materials. Interface boundaries between different materials always occur at control volume boundaries, midway between grid points. Each material used in the construction of the tank is awarded a numerical value to identify the detailed material composition of the tank.

Governing and finite difference equations

The partial differential equation describing heat transfer in the structure of a liquid gas tank, is the three-dimensional, unsteady, conductive heat transfer equation. In cylindrical co-ordinates the equation is:

$$\frac{1}{r}\frac{\partial}{\partial r}\left(rk\frac{\partial T}{\partial r}\right)+\frac{1}{r}\frac{\partial}{\partial \phi}\left(k\frac{\partial T}{\partial \phi}\right)+\frac{\partial}{\partial z}\left(k\frac{\partial}{\partial z}\right)=\rho C\frac{\partial T}{\partial \tau} \tag{1}$$

The finite difference equations used in the numerical procedure are derived by integrating the partial differential equation (1) over control volumes surrounding the grid points[7]. The general

finite difference equation for (1) can be written as:

$$a_p T_p = \sum a_{np} T_{np} + a_p^0 T_p^0 + b \tag{2}$$

The coefficient a_p refers to the central grid point and a_{np} to the neighbouring grid points, while a_p^0 refers to the central point at the previous time interval. The numerical value of the constants depend on the material properties, grid dimensions and the time step used in the solution procedure. At the boundaries of the tank the term b and the coefficient a_p in (2) contain information on the different heat transfer boundary conditions.

Boundary conditions

The numerical model accounts for heat transfer in the form of radiation from the sun, as well as radiative and convective heat transfer with the environment. These boundary heat transfer processes are accounted for in the modelling procedure by imposing the following boundary conditions.

Convection boundaries. The general finite difference equation (2) is also valid at the convective boundaries of the tank. Natural convection is assumed to occur at all these boundaries. In this case, the coefficient a_p contains information on the convective heat transfer coefficient, while the term b contains information on the surrounding fluid temperature and the heat transfer coefficient. The convective heat transfer coefficient is defined by Newton's law of cooling. The equation used to calculate the heat flux at each boundary grid point is:

$$Q = hA(T_s - T_\infty) \tag{3}$$

Vertical surfaces. For the sides of the tank, the natural convective heat transfer coefficient between the steel walls of the tank and the surroundings, is calculated from the following empirical equation[8]:

$$Nu = C_c(Gr_f Pr_f)^m \tag{4}$$

For vertical cylinders the equation is valid if the thickness of the thermal boundary layer is relatively small compared with the diameter of the cylinder. For $GrPr$ numbers from 10^9 to 10^{13} the constants C_c and m were taken as 0.10 and 0.33, respectively[8]. The following equation is then used to calculate the mean heat transfer coefficient $\bar{h}$ on the surface:

$$\bar{h} = \frac{Nu \cdot k}{l} \tag{5}$$

where l is the characteristic dimension.

Horizontal surfaces. The natural convective heat transfer coefficients for the top and bottom surfaces of the tank are also calculated from (4). For the top surface the coefficients used for C_c and m were 0.27 and 0.25 respectively, while values of 0.15 and 0.33 were used for the bottom of the tank which is mounted on pillars 1 m above ground level. The average heat transfer coefficients for these two surfaces are calculated from (6) and (7) where l is the characteristic dimension and d the diameter of the tank.

$$\bar{h} = \frac{Nu \cdot k}{l} \tag{6}$$

$$l = 0.9d \tag{7}$$

Solar radiation boundaries. Due to the outdoor location, the liquid gas tank is exposed to

solar radiation. The intensity of the radiation is strongly dependent upon the location of the tank, the atmospheric conditions, time of year and effective surface area. Published values of time varying solar radiation intensities for the location of the tank[9] were used to determine the solar radiation heat transfer to the surface of the tank. Different data sets were used for the top surface and for each surface facing the four main wind directions. The heat transfer is calculated from:

$$Q = GA\varepsilon \tag{8}$$

In the above equation ε represents the emissivity of the outside surface of the tank which was taken as 0.16 for light colour paints. G represents the solar radiation intensity obtained from Reference 9 and A the surface area.

Radiation boundaries with the environment. Using the concept of a radiation heat transfer coefficient, the effect of radiative heat transfer with the environment can be treated in a similar way as convection heat transfer. The heat transfer coefficient can be defined as:

$$h_r = \frac{(T_S^2 + T_\infty^2)(T_S + T_\infty)}{[(1 - \varepsilon_S)/\varepsilon_S] + (1/F_{S\infty})} \tag{9}$$

where T_S is the wall temperature of the tank, T_∞ the ambient temperature, ε_S the surface emissivity of the tank and $F_{S\infty}$ the geometric view-factor which is unity in this case[10].

The equation for radiative heat transfer with the environment this reduced to:

$$Q = h_r A(T_S - T_\infty) \tag{10}$$

Interface conduction. Interface conduction occurs in the structure of the tank between two different materials which are in contact. The grid was generated in such a way that interfaces between different materials occur at control volume surfaces, midway between grid points. Equation (2) can then be used to calculate the heat transfer at the interface between these two materials. The interface conductivity value between the two materials in contact is obtained from the harmonic mean of the conductivity values of the two materials. The harmonic mean formulation for the interface conductivity k_{int} between materials (1) and (2) is:

$$k_{\text{int}} = 2k_1k_2/(k_1 + k_2) \tag{11}$$

If there is a significant difference between the conductivity values of the two materials in contact, the harmonic mean formulation gives a better description of the interface conductivity than the arithmetic mean[7]. This is of special importance at contact surfaces between Perlite and steel.

In this study the assumption was made that the contact at the interface between the different materials is perfect. This is an acceptable assumption as it results in a higher heat flux and therefore a lower efficiency of the insulation material around the inner gas tank.

Liquid–metal interface. At the interface between the liquid and steel wall heat is transferred to the liquid. The vapour that results from this heat transfer is then released to the atmosphere and the tank is refilled with liquefied nitrogen. Due to this process the temperature throughout the liquid and specifically at the interface is maintained at a constant temperature of −196°C. Therefore a constant temperature boundary was assumed.

SOLUTION OF THE GRID

Owing to the cyclic environmental conditions, the temperature distribution and heat flux in a liquid gas tank varies greatly over a twenty-four hour period. For the purpose of this study a

steady state temperature distribution through the tank was initially assumed. From here, the solution was allowed to progress in time steps of ten seconds. The Gauss–Seidel iteration scheme was used to solve the finite difference equations (2) at each time step. The solution was fully converged at each time step before moving to the next. Convergence at each time step is assumed if the cumulative temperature difference over the grid differs by so little from the distribution of the previous iteration that it does not influence the accuracy of the solution. This real time simulation was continued until the predicted temperature distribution did not differ at any time of the day from the temperature simulated for the same time the previous day. For this tank configuration it was found to be the twenty-four hour period between 72 and 96 hour real time from starting the simulation.

RESULTS AND DISCUSSION

The aim of effective insulation material is to reduce the heat flux to the liquid gas inside the tank by phasing out the large variations in heat flux entering the tank over a twenty-four hour period. In *Figure 2* the heat flux through the outside wall of the tank is compared with the heat flux that reaches the liquid gas over a twenty-four hour period on a typical summer's day. After 6 a.m. heat is transferred to the tank as a result of solar radiation and increasing ambient temperature. As the surface temperature of the tank increases above the ambient temperature, heat is transferred from the tank to the environment in the form of convection and radiation. This opposes radiative heat transfer from the sun to the tank and reduces the overall heat flux to the tank. During the afternoon the intensity of the solar radiation decreases which leads to a reduction in the heat flux through the surface. After 4 p.m. the convective and radiative losses to the environment exceed gains from solar radiation. The net heat transfer to the tank thus becomes negative. This negative heat flux to the tank continues until 6 a.m. the next morning. The heat transferred to the liquid over a twenty-four hour period is therefore the sum of the positive and negative heat flux through the wall.

The heat flux through the inner tank to the liquid gas is, however, constant. The insulation material used in this simulation therefore effectively dampens the fluctuating heat flux through the wall. Furthermore, the fluctuation of the wall temperature has a relatively small influence on the resultant heat transfer to the liquid gas, as this fluctuation is small when compared with the total temperature difference between the liquid and the ambient temperature.

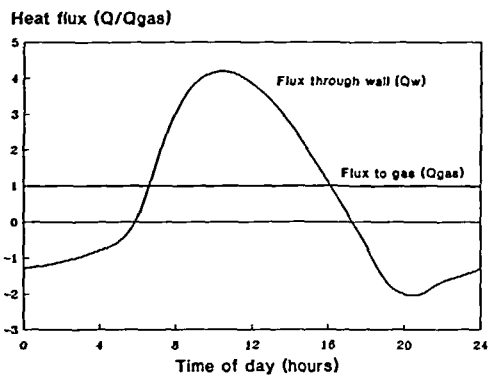

Figure 2 24 Hour cycle of heat flux through outer and inner tanks

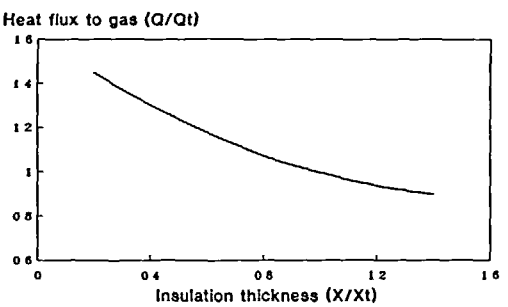

Figure 3 Heat flux to liquid as a function of insulation material thickness

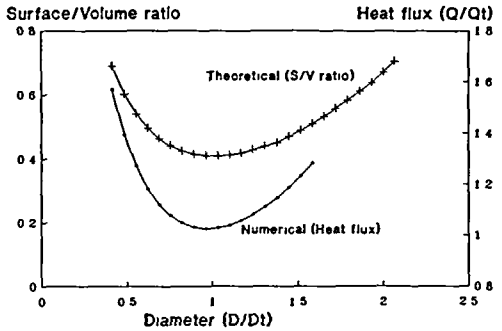

Figure 4 Heat flux and surface-to-volume ratio for different configurations of a 2477 m^3 tank

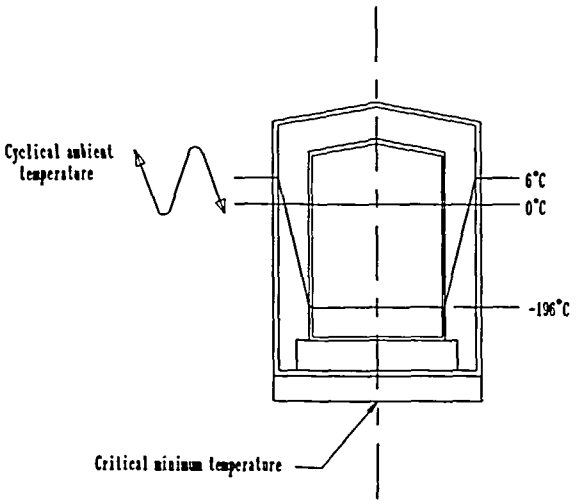

Figure 5 Temperature distribution at 2400 h

The most important parameter influencing the rate of heat transfer to the tank is the thickness of the insulation material. The material is, however, also expensive and therefore the main contribution to the capital cost of erecting such a tank. It is therefore important to investigate the effect of insulation thickness on the heat flux to the tank. *Figure 3* shows the relation between the heat flux that reaches the liquid gas and the thickness of the insulation material (Perlite). It applies specifically to a liquid gas tank with an inner tank diameter of 13.35 m and a height of 18 m. For this 2477 m^3 tank, filled with liquid nitrogen at $-196°C$, the insulation thickness varied from 0.4 to 1.4 m. The Figure indicates how the heat flux reaching the liquid gas decreases as the insulation thickness increases. From this Figure accurate quantitative information can be obtained that is essential for the optimization of the design of gas tanks. This result, together with the economic implications, can be used to determine the optimum insulation thickness for the liquid gas tank.

With the insulation material thickness known, the next step in the design process of the tank is to optimize the shape of the tank. The shape is optimized when the heat flux to the liquid gas is minimized. The theoretical optimum shape is obtained when the surface-to-volume ratio is a minimum. *Figure 4* exhibits the area-to-volume ratio as a function of the tank diameter. From this the optimal theoretical diameter for a 2477 m^3 tank is found to be 14.5 m.

Figure 4 also displays the relation between total heat flux and tank diameter. The total heat flux is made up of the sum of the heat flux through all the different surfaces of the tank. For an insulation thickness of 1.2 m the various heat flux values are: top, 5.86; side, 5.79; bottom: 9.29 W/m^2.

The heat flux differs as a result of differences in boundary conditions at the surfaces. Knowledge of these fluxes is used to thermally optimize the shape of the tank (2477 m^3). From *Figure 4* the diameter of the thermally optimized tank is found to be 13.5 m. This differs from the theoretical optimum diameter of 14.5 m, which did not take into account the variation in heat flux through the different surfaces. The real optimum tank diameter is therefore 13.5 m.

Apart from calculating the heat flux, the model also predicts the temperature distribution throughout the tank. *Figure 5* shows the temperature distribution through the centre of the tank at 2400 h on a typical summer's day. The temperature distribution in the tank is calculated at each time step and is therefore available for any time of the day.

CONCLUSIONS

The numerical modelling of the gas tank provides complete information on the temperature distribution and heat flux in the tank. From the temperature distribution in the tank it can be determined whether or not embrittling or crumbling of the concrete slab can occur. Edge temperatures and especially the temperature at the bottom of the concrete slab can be predicted to determine whether the accumulation of ice at that point is possible. The knowledge of the heat flux to the gas tank is used to predict the thermal performance of the gas tank. From this information the percentage evaporation losses are calculated. If the numerical simulation predicts that any of the above mentioned requirements will not be met, the design of the gas tank can be altered until the tank complies with the set limits. Heat fluxes through the different surfaces of the gas tank are determined and used to optimize the tank geometry for a certain volume and fixed insulation material thickness.

With the proposed procedure it is now possible to model any size and shape of gas tank for any environmental conditions. A useful tool when designing and optimizing gas tanks is therefore supplied.

REFERENCES

1 Sunden, B. A numerical investigation of the transient temperature distribution in a three-layered solid with time-varying boundary conditions, *Numerical Methods in Thermal Problems*, Vol. 6, Part 1, Pineridge Press, Swansea, pp. 111–119 (1989)
2 Sunden, B. Numerical prediction of transient heat conduction in a multi-layered solid with time-varying surface conditions, *Numerical Methods in Thermal Problems*, Vol. 5, Part 1, Pineridge Press, Swansea, pp. 207–218 (1987)
3 Claes, L. Determination of temperature gradients in a circular concrete shaft. *Numerical Methods in Thermal Problems*, Vol. 5, Part 2, Pineridge Press, Swansea, pp. 1518–1529 (1987)
4 Fu, H. C., Ng, S. F. and Cheung, M. S. Temperature distributions on concrete-steel composite bridges, *Numerical Methods in Thermal Problems*, Vol. 6, Part 1, Pineridge Press, Swansea, pp. 202–215 (1989)
5 Van der Walt, J. C., Visser, J. A. and Mathews, E. H. Numerical simulation of the heat transfer in and around a steel bar during reheating and hot rolling, *Numerical Methods in Thermal Problems*, Vol. 6, Part 1, Pineridge Press, Swansea, pp. 1456–1565 (1989)
6 Visser, J. A. A two-dimensional numerical model for predicting temperature distribution in a casting channel, *Technical Report*, Dept. of Mech. Eng., University of Pretoria (1989)
7 Patankar, S. V. *Numerical Heat Transfer and Fluid Flow*, Hemisphere, New York (1980)
8 Holman, J. P. *Heat Transfer*, Sixth edition, McGraw-Hill, Singapore (1981)
9 Van Deventer, E. N. Climatic and other design data for evaluating heating and cooling requirements of buildings, *CSIR Research Report 300*, Pretoria (1971)
10 Visser, J. A. The numerical prediction of temperature distribution in steel billets during hot rolling, *MEng Thesis*, Dept. of Mech. Eng., University of Pretoria (1986)